

Supplement of Atmos. Chem. Phys., 18, 12363–12389, 2018
<https://doi.org/10.5194/acp-18-12363-2018-supplement>
© Author(s) 2018. This work is distributed under
the Creative Commons Attribution 4.0 License.



Supplement of

Aerosol distribution in the northern Gulf of Guinea: local anthropogenic sources, long-range transport, and the role of coastal shallow circulations

Cyrille Flamant et al.

Correspondence to: Cyrille Flamant (cyrille.flamant@latmos.ipsl.fr)

The copyright of individual parts of the supplement might differ from the CC BY 4.0 License.

Comparison between WRF dynamics at 2-km, aircraft and radiosounding observations

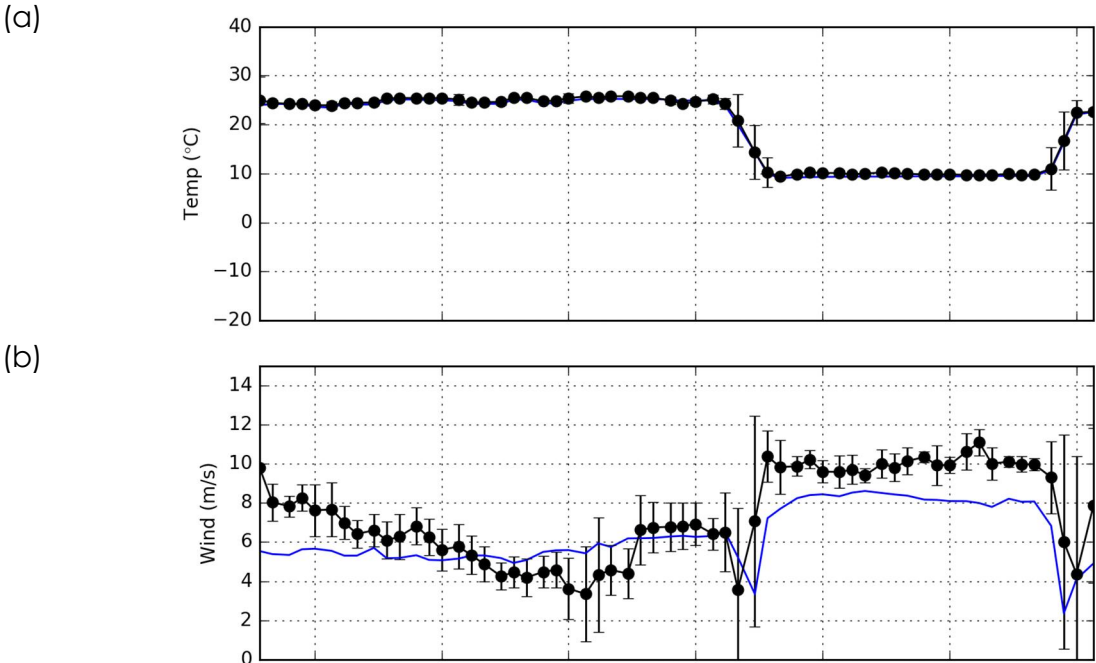


Figure S1: Evolution of temperature (a) and wind speed (b) along the ATR 42 flight track for in situ observations (closed black circles) and WRF (blue solid line). The mean value and standard deviation of the observations within WRF grid cells are indicated as dots and whiskers, respectively.

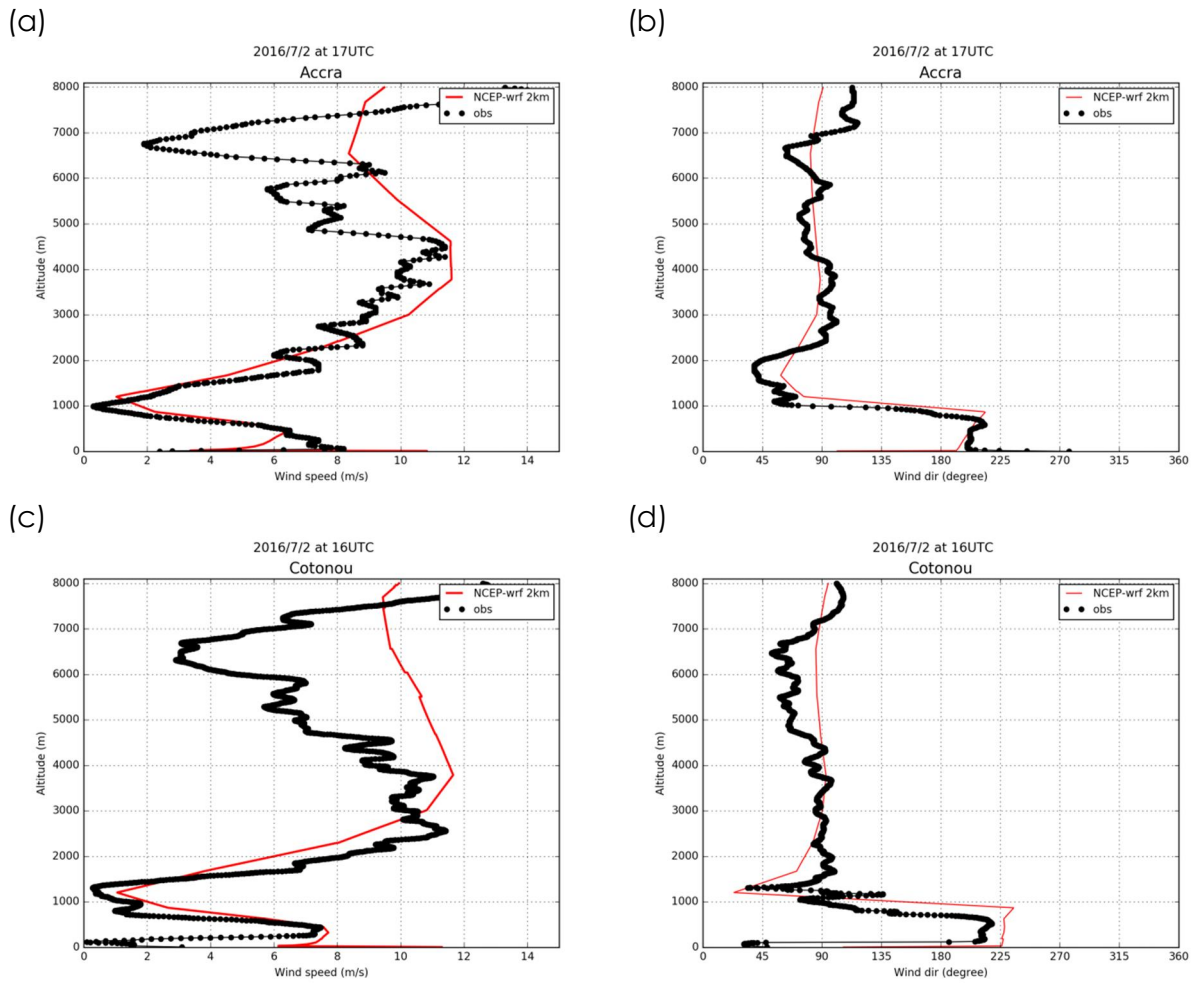
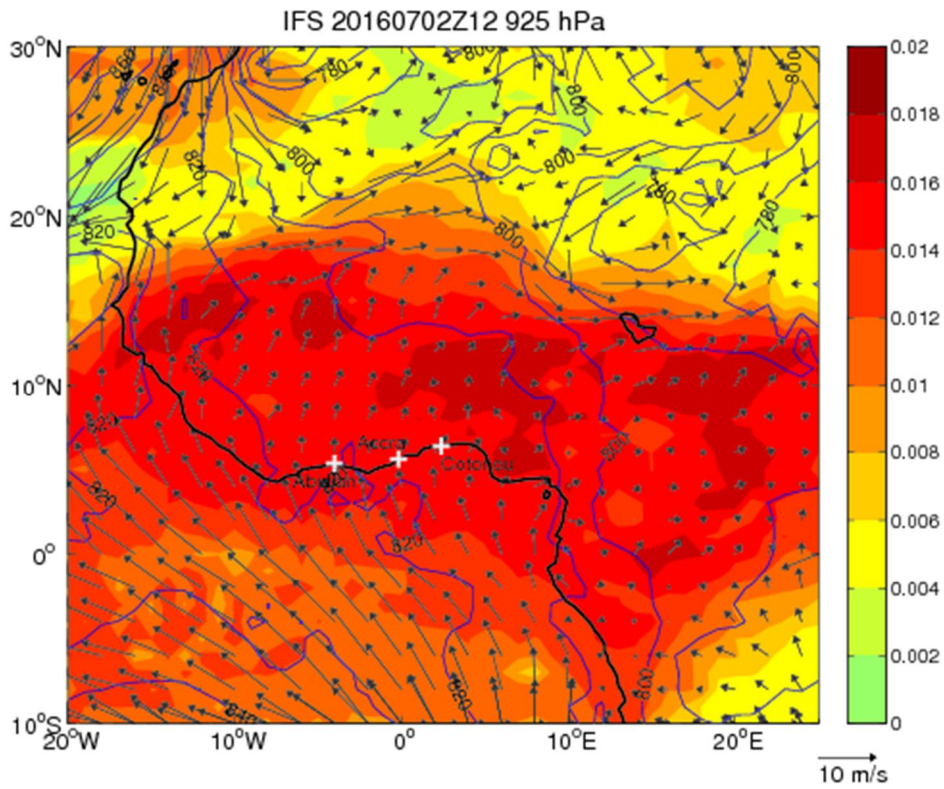


Figure S2: Wind speed (left column) and wind direction profiles (right column) in Accra (a and b, respectively) and Cotonou (c and d, respectively). Observations are shown as black dots and 2-km WRF simulations are shown as red solid lines. The radiosoundings were released at 1700 and 1612 UTC in Accra and Cotonou, respectively.

Regional scale dynamics from IFS

(a)



(b)

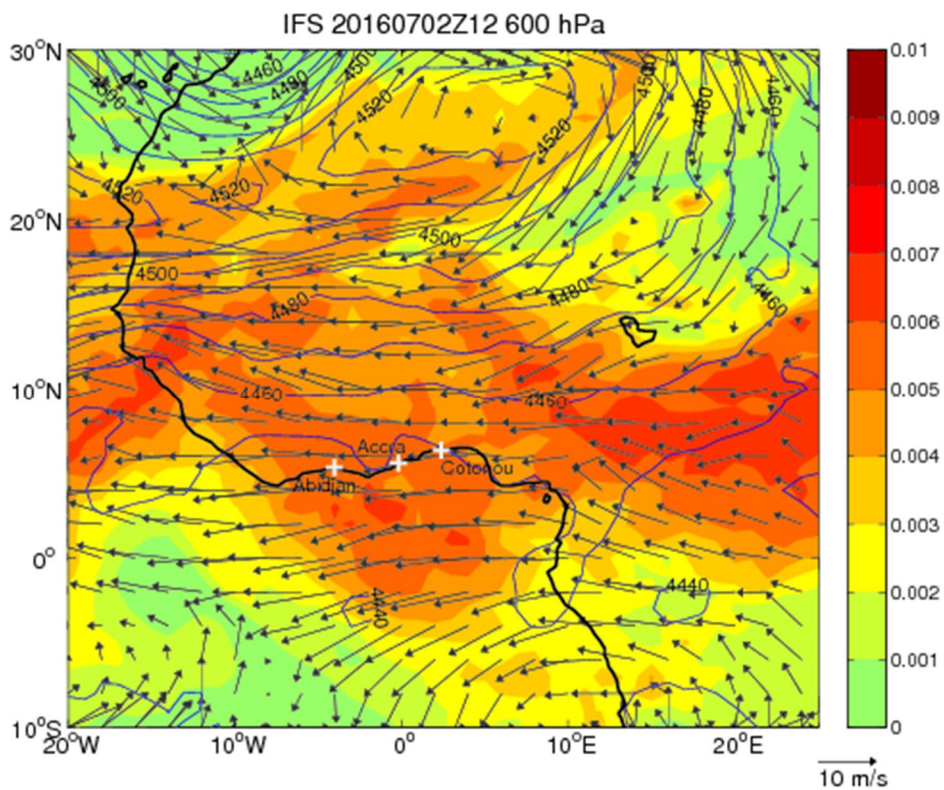


Figure S3: ECMWF IFS analyses at 1200 UTC on 2 July for water vapor mixing ratio (kg kg^{-1} , color shading), wind (vectors) and geopotential height (m, blue solid lines) at (a) 925 hPa and (b) 600 hPa. The African continent coastline is shown as a black solid line and cities of interest are indicated.

Regional scale aerosol composition from IFS-CAMS

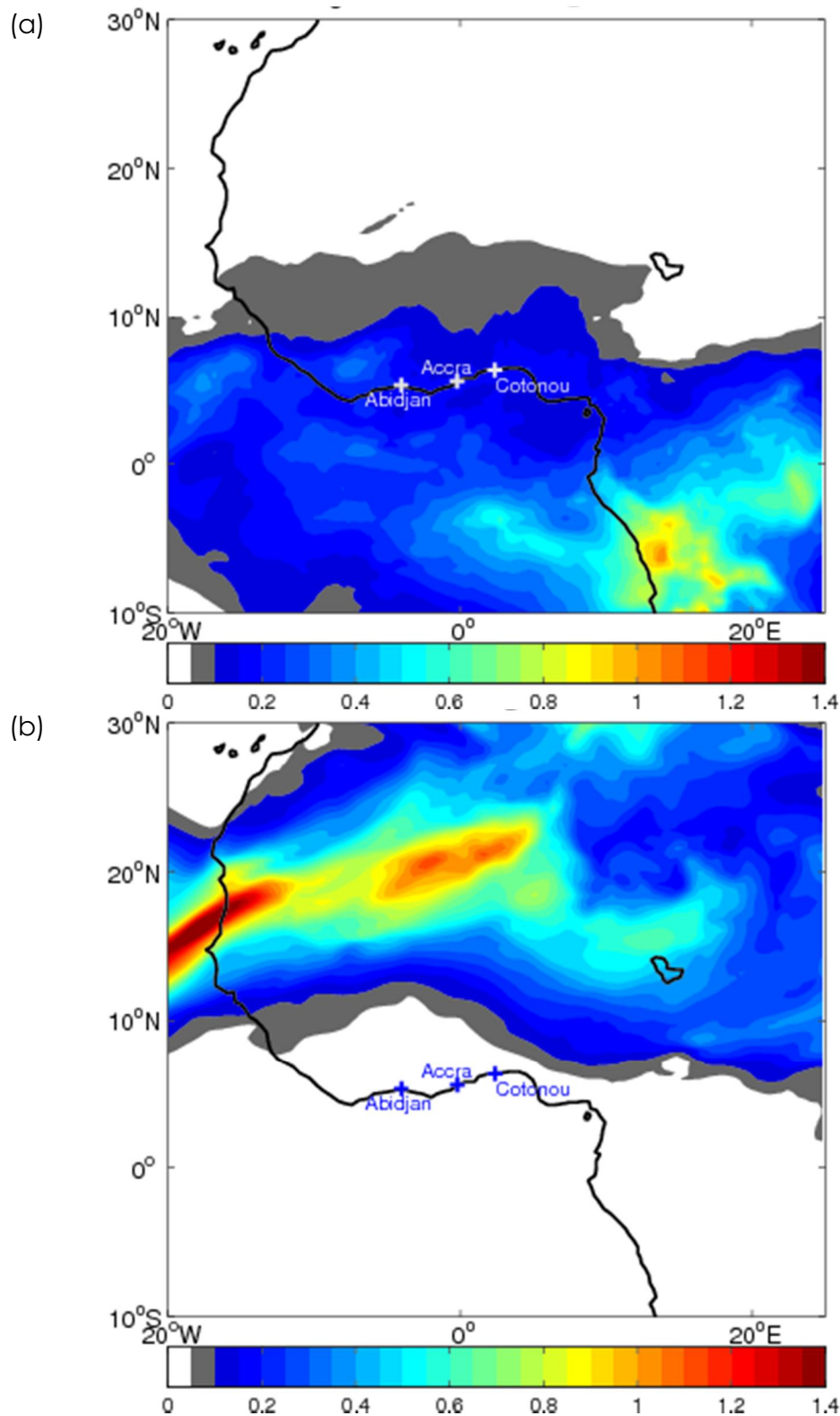


Figure S4: ECMWF CAMS forecast on 2 July 2016 at 1200 UTC (+12h forecast) for (a) organic matter AOD and (b) dust AOD. The African continent coastline is shown as a black solid line and cities of interest are indicated.

Regional overturning circulation induced by land-sea skin temperature gradients

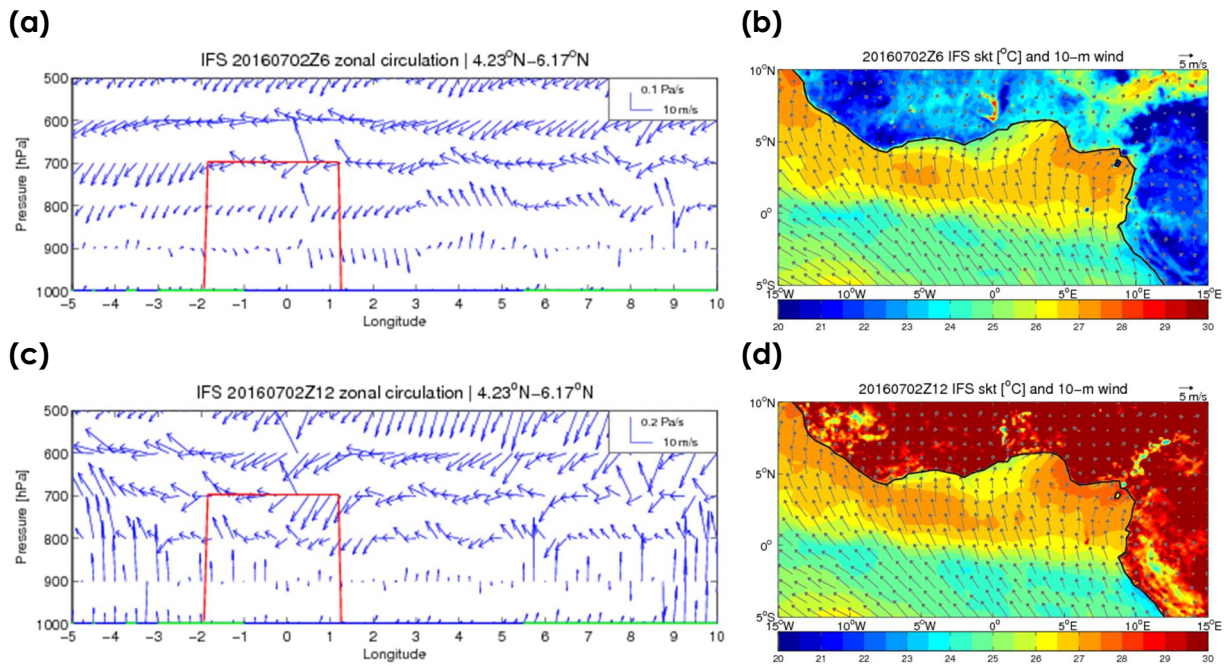


Figure S5: Left column: West–east oriented vertical cross section (1000–500 hPa) of zonal-vertical wind vectors from IFS analyses (blue) between 5°W and 10°E averaged between 4.54°N and 6.28°E at (a) 0600 and (c) 1200 UTC on 2 July 2016. The thick red line is the projection of the ATR 42 aircraft track onto the cross-section. The thick green and blue lines at the bottom of the graph indicate the presence of land and ocean, respectively. Surface characteristics are defined based on the dominating surface type in the latitudinal band considered for the average of the wind field. Right column: IFS skin temperature (colors) and wind field at 10 m (vectors) at (b) 0600 UTC and (d) 1200 UTC. Cross-sections (a) and (c) are computed in the zonal box shown in **Figure 12c** of the main paper.

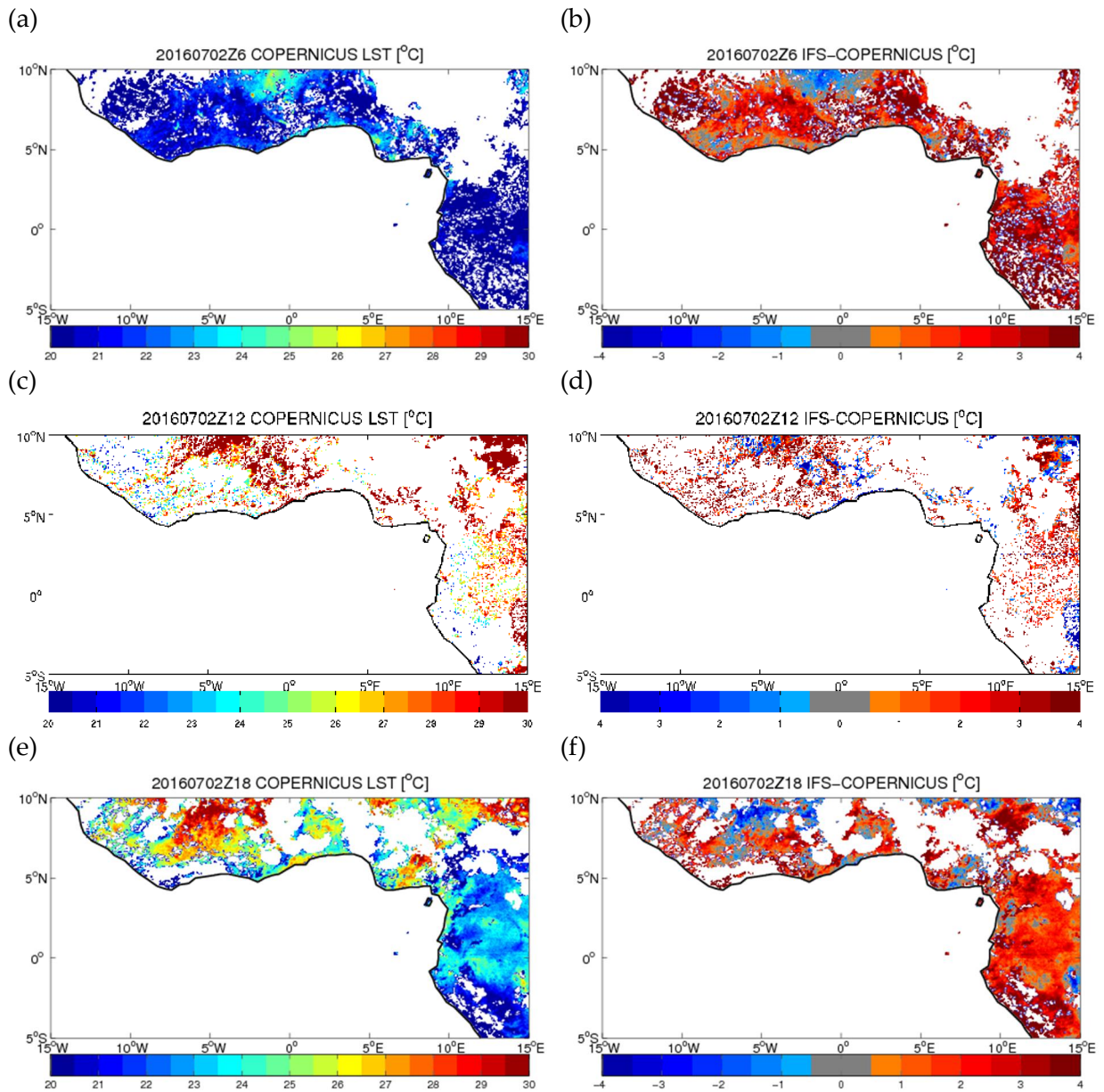


Figure S6: Left column: Copernicus skin temperature at (b) 0600 UTC, (d) 1200 UTC and (f) 1800 UTC on 2 July 2016. Right column: IFS minus Copernicus skin temperature at (b) 0600 UTC, (d) 1200 UTC and (f) 1800 UTC. IFS skin temperature, originally at 0.125° resolution, has been linearly interpolated onto the Copernicus grid at 5 km before computing the differences.

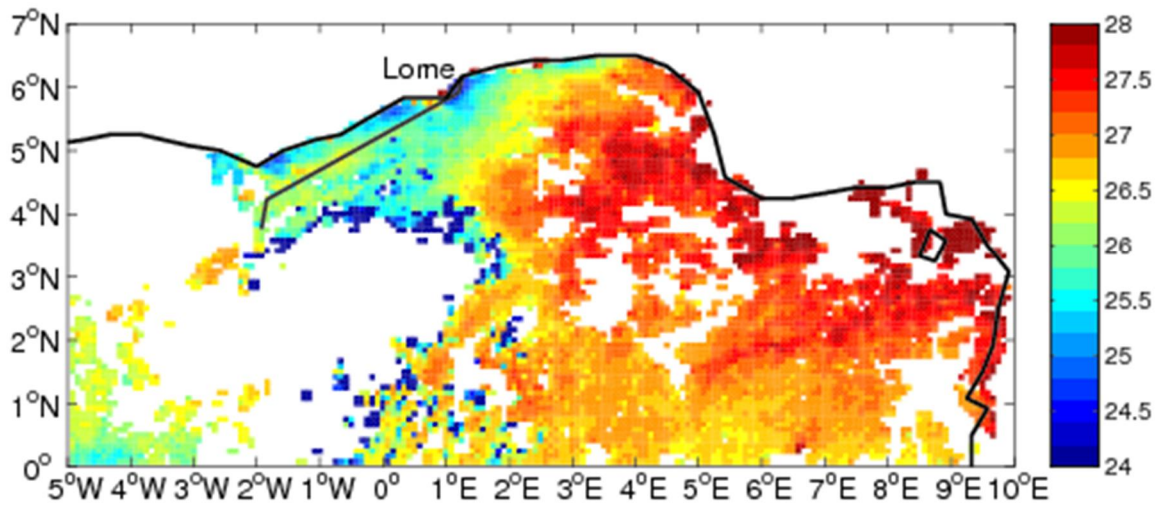


Figure S7: MODIS-derived SST on 2 July 2016, with superimposed ATR 42 flight track (black thick line).